Submitted to Phys. Rev. D for publication, July 1994
Preprint Bern BUHE-94-6

Energy transport via quasiparticle and phonon propagation in Superheated Superconducting Granule detectors after nuclear recoils.

A. Gabutti *
Laboratory for High Energy Physics, University of Bern,
Sidlerstrasse 5, CH 3012 Bern, Switzerland

Abstract

The propagation of the excess of quasiparticles and phonons produced by a nuclear recoil inside superheated superconducting granules will be discussed. The decay towards equilibrium of the initial disturbance is assumed to be a thermal diffusion process described by a set of coupled heat flow equations for the effective quasiparticle and phonon temperatures. The solution is carried out analytically for a point source located anywhere inside the superconducting granule with the initial energy distributed in both quasiparticle and phonon systems. The calculated sensitivity to nuclear recoils and the delay in time between interaction and phase transition are compared with irradiation measurements performed on Sn and Zn granules. The derived expressions for the quasiparticle and phonon temperatures are useful to predict the sensitivity of SSG detectors to nuclear recoils produced in dark matter particle or neutrino interactions.

PACS numbers: 95.30.C, 07.62

* present address:
Max-Planck-Institut für Physik, D-8000 München 40, Germany

1 Introduction

Superheated Superconducting Granule (SSG) detectors consist of a collection of tiny metastable superconducting granules embedded in a dielectric material. The granules are kept in the superconducting state at a constant temperature in an applied magnetic field below the superheating field. The energy deposited by the interacting particle rises the granule temperature above the transition temperature and the detection principle is based on the measurement of the phase transition from the superconducting to the normal conducting state. The disappearance of the Meissner effect due to the phase transition produces a change in the magnetic flux which is measured using a pick-up coil wounded around the detectors. A large number of granules ($\sim 10^6$) can be read out with a single pick up coil sensitive to the transition of individual granules. A review of the SSG detector development can be found in Ref. [1].

SSG detectors are being presently developed for cold dark matter detection [2]. Weakly interacting massive particles can be detected measuring the recoil energy released when they interact with a nucleus inside the granule via neutral-current exchange. The expected nuclear recoil energies are in the range 1-100 keV with a seasonal modulation in the detection rate depending on the mass of the dark matter particles [3].

The sensitivity of Sn, Al and Zn granules to nuclear recoils of few keV has been measured by irradiating SSG detectors with a 70 MeV neutron beam [4]. In the case of Al and Zn SSG, the irradiation measurements have shown that the detector energy threshold can be evaluated considering the energy needed to rise the temperature of the whole granule from the bath to the transition temperature (referred as *global heating model*). On the contrary, the measured energy threshold of Sn granules was almost a factor of two lower than predicted by the global heating model. This effect was also found in irradiation experiments with minimum ionizing particles [5] and radioactive sources [6]. The enhanced sensitivity of Sn granules has been related [7] to the possibility of producing a phase transition when only a small portion of the granule surface is heated above the transition temperature (referred as *local heating model*).

Irradiation tests of SSG detectors with a 70 MeV neutron beam have also been used to study the delay in time between the neutron elastic scattering and the phase transition of a single granule inside the detector. Typical delay times of $\sim$100 ns and $\sim$500 ns have been measured in SSG made of 15-20 μm Sn and 28-30 μm Zn granules respectively [8].

In the present work we will consider the energy transport inside superheated superconducting granules after nuclear recoils. The occurrence of global or local heating and the delay in time between nuclear recoils and phase transitions will be discussed in the case of Sn and Zn superconducting granules.

After a nuclear elastic scattering, the deposited energy is transferred to electrons

and to the lattice by the recoiling nucleus. The initial disturbance is localized at the interaction point and produces an excess of quasiparticles and phonons in a state very far from equilibrium where the kinetic energy of the quasiparticles is larger than kT_c. After a few *ps* this hot electron gas exhibits a local equilibrium with the phonons and a slower relaxation process dominated by heat diffusion takes place [9].

The decay towards equilibrium of the initial disturbance is assumed to be a thermal diffusion process described by a set of coupled heat flow equations for the effective quasiparticle and phonon temperatures. The solution is carried out analytically for a point source located anywhere inside the superconducting granule with the initial energy distributed in both quasiparticle and phonon systems.

The heat propagation in superconducting spheres is discussed in Ref. [10] for an ionizing particle depositing energy only in the quasiparticle system as a primary excitation. These results can not be applied to the case of nuclear recoils where a large fraction of the energy is transferred to the phonons as a primary excitation.

2 Thermal Diffusion

The decay towards equilibrium of the initial disturbance is described by a set of coupled heat flow equations [10, 11] for the effective quasiparticle (T_e) and phonon temperatures (T_p):

$$\begin{aligned} \frac{\partial T_e}{\partial t} &= D_e \nabla^2 T_e - \frac{1}{\tau_e}(T_e - T_p) + A_e \delta_e(\vec{r_o}, t_o) \\ \frac{\partial T_p}{\partial t} &= D_p \nabla^2 T_p - \frac{1}{\tau_p}(T_p - T_e) + A_p \delta_p(\vec{r_o}, t_o) \end{aligned} \tag{1}$$

where D_e and D_p are the thermal diffusivities, τ_e and τ_p the quasiparticle and phonon lifetimes and T_b the bath temperature. The initial disturbance is assumed to be a point source in $\vec{r_o}$ at the time t_o described by the delta functions $\delta_e(\vec{r_o}, t_o)$ and $\delta_p(\vec{r_o}, t_o)$ with A_e and A_p accounting for the initial energy share between the two systems.

In SSG detectors, the granules are embedded in a dielectric material (typically plasticine or Al_2O_3 powder) and the heat transfer to the bath is due only to phonons crossing the granule surface . The characteristic time for this process can be evaluated using the acoustic mismatch model for a spherical boundary [10, 12]. The resulting time is of the order of few μs which is much longer than the time scale of the relaxation processes (see Sec. 3) and is neglected in the calculations.

Eq. (1) can be solved analytically using Fourier transforms and the eigenvalues method [13] with the thermal diffusivities and the carrier lifetimes being independent of temperature. The spatial eigenfunctions of the solution are the even and odd spherical harmonic functions:

$$\Psi^e_{m,n,l}(\vec{r}) = \frac{1}{\Lambda} cos(m\phi) j_n(k_{l,n}\frac{r}{a}) P^m_n(cos\theta) \qquad (2)$$
$$\Psi^o_{m,n,l}(\vec{r}) = \frac{1}{\Lambda} sin(m\phi) j_n(k_{l,n}\frac{r}{a}) P^m_n(cos\theta)$$

where j_n are the spherical Bessel function of order n and and P the associated Legendre Polynomes of order m. The normalization constant Λ is derived from the orthogonality of the eigenfunctions [13]:

$$\Lambda^2 = \frac{2\pi a^3}{\epsilon_m(2n+1)} \frac{(n+m)!}{(n-m)!} \Big[1 - \frac{n(n+1)}{k^2_{l,n}}\Big] j^2_n(k^2_{l,n}) \qquad (3)$$

where the Neumann factor ϵ_m=1 for n=0 and ϵ_m=2 for n=1,2,....

The general form of the solution is a linear combination of even and odd spherical harmonics:

$$T_e(\vec{r},t) = \sum_{m=0}^{\infty}\sum_{n=0}^{\infty}\sum_{l=0}^{\infty} \Big[\Psi^e_{m,n,l}(\vec{r}) + \Psi^o_{m,n,l}(\vec{r})\Big] \frac{1}{2\pi} \int_{-\infty}^{\infty} e^{i\omega t} \tilde{T}_e(\omega, l)\, d\omega \qquad (4)$$

where $\tilde{T}_e$ is the Fourier transform of T_e. A similar expression holds for the phonon temperature with T_p instead of T_e. The coefficients $k_{l,n}$ are derived from the positive roots of the Neumann boundary conditions at the granule surface ($r = a$) [10]:

$$\Big(\frac{\partial T_e}{\partial r}\Big)_{r=a} = \Big(\frac{\partial j_n(k_{l,n}\frac{r}{a})}{\partial r}\Big)_{r=a} = 0 \qquad (5)$$

which states that the quasiparticles do not contribute to the heat transfer to the bath.

The time dependent part of the solution is obtained substituting in Eq. (1) the temperatures and the initial perturbation with the corresponding eigenfunctions:

$$\begin{aligned} T_e(\vec{r},t) &\rightarrow \Psi_{m,n,l}(\vec{r}) e^{i\omega t} \tilde{T}_e(\omega, l) \\ \delta_e(\vec{r_o}, t_o) &\rightarrow \Psi_{m,n,l}(\vec{r}) e^{i\omega t} \tilde{\delta}_e(\omega, l) \end{aligned} \qquad (6)$$

and similar expression for the phonons system. After substitution, the coupled diffusion equation becomes:

$$\begin{aligned} (i\omega + D_e x^2_{l,n})\tilde{T}_e &= -\frac{1}{\tau_e}(\tilde{T}_e - \tilde{T}_p) + A_e\tilde{\delta}_e \\ (i\omega + D_p x^2_{l,n})\tilde{T}_p &= -\frac{1}{\tau_p}(\tilde{T}_p - \tilde{T}_e) + A_p\tilde{\delta}_p \end{aligned} \qquad (7)$$

with $x_{n,l}$=$k_{l,n}/a$. The system eigenfrequencies ($\omega_\pm$) are derived from Eq. (7) considering the case of a zero initial perturbation (A_e=A_p=0) and are:

$$\omega_\pm = \frac{i}{2}\Big\{(D_e + D_p)x^2_{l,n} + \frac{1}{\tau} \mp \sqrt{\Big[\frac{1}{\tau} - (D_e - D_p)x^2_{l,n}\Big]^2 + \frac{4}{\tau_e}(D_e - D_p)x^2_{l,n}}\Big\} \qquad (8)$$

with:

$$\frac{1}{\tau} = \left(\frac{1}{\tau_e} + \frac{1}{\tau_p}\right) \tag{9}$$

The expressions of $\tilde{T}_e$ and $\tilde{T}_p$ in the case of a non zero initial perturbation depend on the eigenfrequencies $\omega_\pm$ and are derived solving Eq. (7). After partial fraction reduction we have:

$$\tilde{T}_e = \frac{1}{(i\omega - \alpha_+)^2 - \alpha_-^2}\left[A_e\tilde{\delta}_e(i\omega + \beta) + \frac{A_p\tilde{\delta}_p}{\tau_e}\right] \tag{10}$$

$$\tilde{T}_p = \frac{1}{(i\omega - \alpha_+)^2 - \alpha_-^2}\left[A_p\tilde{\delta}_p(i\omega + \gamma) + \frac{A_e\tilde{\delta}_e}{\tau_p}\right]$$

where:

$$\alpha_\pm = \frac{i}{2}(\omega_+ \pm \omega_-) \quad , \quad \beta = D_p x_{l,n}^2 + \frac{1}{\tau_p} \quad , \quad \gamma = D_e x_{l,n}^2 + \frac{1}{\tau_e} \tag{11}$$

Considering a diffusion process starting at t_o=0, the Fourier transform of the initial disturbance is given by:

$$A_e\tilde{\delta}_e = T_e^\star \int_{-\infty}^{\infty} e^{-i\omega t}\delta(t_o)\,dt \int \left(\Psi_{m,n,l}(\vec{r})\right)^* \delta(\vec{r_o})\,d\vec{r} = T_e^\star \Psi_{m,n,l}(\vec{r_o}) \tag{12}$$

where $T_e^\star$ is the initial temperature of the quasiparticle system due to the energy loss by the interacting particle. A similar expression holds for $A_p\tilde{\delta}_p$ with $T_p^\star$ instead of $T_e^\star$.

The phonon and quasiparticle temperatures are then evaluated substituting in Eq. (4) the obtained expressions for $\tilde{T}_e$ and $\tilde{T}_p$. After integration we have:

$$\begin{aligned} T_e(\vec{r},t) &= T_b + F_e(t) \\ &\quad + V\sum_{m=0}^{\infty}\sum_{n=0}^{\infty}\sum_{l=1}^{\infty}\left[\Psi^e_{m,n,l}(\vec{r})\Psi^e_{m,n,l}(\vec{r_o}) + \Psi^o_{m,n,l}(\vec{r})\Psi^o_{m,n,l}(\vec{r_o})\right]F_e(l,t) \end{aligned} \tag{13}$$

with V the granule volume. A similar expression holds for the phonon temperature $T_p(\vec{r},t)$ with F_p instead of F_e. The time dependent part of the quasiparticle (F_e) and phonon (F_p) temperatures are:

$$F_e(l,t) = \frac{1}{i(\omega_+ - \omega_-)}\left\{\left[T_e^\star(\beta + i\omega_+) + \frac{T_p^\star}{\tau_e}\right]e^{i\omega_+ t} - \left[T_e^\star(\beta + i\omega_-) + \frac{T_p^\star}{\tau_e}\right]e^{i\omega_- t}\right\}$$

$$F_p(l,t) = \frac{1}{i(\omega_+ - \omega_-)}\left\{\left[T_p^\star(\gamma + i\omega_+) + \frac{T_e^\star}{\tau_p}\right]e^{i\omega_+ t} - \left[T_p^\star(\gamma + i\omega_-) + \frac{T_e^\star}{\tau_p}\right]e^{i\omega_- t}\right\} \tag{14}$$

The terms $F_e(t)$ and $F_p(t)$ are calculated from Eq. (14) with l=0 which corresponds to the condition $x_{l,n}$=0.

The derived expressions for T_e and T_p are linear combinations of the initial perturbation in both quasiparticle and phonon systems. Eq. (13) exhibits a mixture of relaxation and diffusion terms and is valid for any interaction point inside the superconducting granule.

3 Initial temperatures and carrier lifetimes

After a nuclear recoil, the deposited energy is transferred to electrons and to the lattice by the recoiling nucleus. The partition of the initial energy is introduced in the final expression for the quasiparticle and phonon temperatures, Eq. (13), by choosing for the initial temperatures $T_e^\star$ and $T_p^\star$ the values:

$$\begin{aligned} T_e^\star &= (T_e^i - T_b) \\ T_p^\star &= (T_p^i - T_b) \end{aligned} \tag{15}$$

The quasiparticle and phonon temperatures T_e^i and T_p^i are evaluated from the integral of the lattice (C_p) and superconducting electrons (C_{es}) specific heats:

$$\begin{aligned} E_r f &= V \int_{T_b}^{T_e^i} C_{es}\, dT \\ E_r(1-f) &= V \int_{T_b}^{T_p^i} C_p\, dT \end{aligned} \tag{16}$$

where f is the fraction of the initial recoil energy E_r transferred to electrons as a primary excitation. The energy share between the two systems depends on the detector material and on the recoil energy. In the present work, the initial temperatures T_e^i and T_p^i after a nuclear recoil were evaluated using the ionization ratio f derived from the simplified expression:

$$f = 0.439\ \epsilon^{-0.173} \tag{17}$$

with:

$$\epsilon = 5.03 \cdot 10^{-4} Z^{-4/3} E_r(eV) \tag{18}$$

obtained from a fit of Fig. 3 of Ref. [14]. Eq. (17) holds for values of the parameter κ=0.133 $Z^{2/3}$ $A^{-1/2}$ $\simeq$0.15 with A the mass number and Z the atomic number of the detector material. Typical values of f in Sn and Zn absorbers (κ=0.16) are $\sim$0.22 and $\sim$0.4 for recoil energies of 5 keV and 100 keV respectively.

The ionization ratios derived from Ref. [14] well fit the values measured in neutron irradiation experiments with Si and Ge diode detectors also at cryogenic temperatures [15]. However this prediction has not been experimentally verified in the case of superconducting materials, where part of the initial energy is transferred to quasiparticles as a primary excitation.

The derived expressions for the quasiparticle and phonon temperatures, Eq. (13), are valid for an initial perturbation localized at the interaction point. This condition is satisfied in the case of nuclear recoils produced by neutral-current scatterings of dark matter particles or in neutron elastic scatterings. The condition f=1 corresponds to an ionizing interaction where the initial energy is deposited only in the quasiparticle system. Eq. (13) with f=1 well approximates the case of soft x-rays absorption

where the emitted photoelectron looses an important fraction of its energy near the interaction point and can also be used to study the thermal propagation in In granules due to the low energetic β^- particle produced in the neutrino nuclear interactions [16]. The derived expressions for the quasiparticle and phonon temperatures can not be used in the case of minimum ionizing particle interactions where the initial energy is released along the particle track.

At the beginning of the diffusion process (t=0) the rise in temperature is localized at the interaction point with T_e and T_p proportional to the partition of the initial energy between the two systems given by the conditions $F_e(0,l) = F_e(0) = T_e^i$ and $F_p(0,l) = F_p(0) = T_p^i$.

The time dependent parts of the solution F_e and F_p, Eq. (14), decay exponentially to zero and at the end of the diffusion process (t=∞) the equilibrium temperatures are T_e=T_p=T_∞. The energy conservation inside the granule impose the conditions:

$$E_r = V \int_{T_b}^{T_\infty} (C_{es} + C_p)\, dT \tag{19}$$

and

$$\frac{\tau_p}{\tau_e} = \frac{T_e^i - T_\infty}{T_\infty - T_p^i} \tag{20}$$

where T_∞ is evaluated considering the rise in temperature of the full granule volume due to the deposited energy E_r. The carrier lifetime ratio defined in Eq. (20) is a function of the recoil energy and of the partition of the initial energy.

The dominant quasiparticles relaxation processes are inelastic scatterings with phonons and recombinations to form Cooper pairs. The resulting lifetime τ_e depends on the temperature and energy of the quasiparticles. During the thermalization process, the excess of energy is exchanged many times between quasiparticles and phonons. After a few phonon generation processes (t ~100 ps), the characteristic energy of the quasiparticles is reduced from an initial value greater then the superconducting energy gap Δ to a value $\sim 2\Delta$ [9].

The lifetimes τ_e and τ_p introduced in Eq. (1) do not depend on the quasiparticle and phonon energies and have to be considered as mean values of the effective energy dependent relaxation times. We evaluated the lifetime τ_e at the temperature T_∞ for quasiparticles of energy 2Δ using the relation:

$$\frac{1}{\tau_e} = \frac{1}{\tau_o}\left[\frac{1}{0.024}\exp\left(\frac{1.76T_c}{T_\infty}\right)\sqrt{\frac{T_\infty}{T_c}} + \left(2\frac{T_\infty}{T_c}\right)^{7/2} + \frac{1}{0.394}\right] \tag{21}$$

derived from Ref. [17] with the superconducting energy gap constant in temperature $\Delta = \Delta_o = 1.76 K_B T_c$ [18]. Eq. (21) holds for recoil energies less than ~100 keV in Zn and Sn where $T_\infty \ll T_c$. The lifetime τ_o depends on the superconducting material and in Sn τ_o=2.3 ns while in Zn τ_o=780 ns [17]. The relaxation processes are much faster in Sn due to the smaller value of the characteristic lifetime τ_o.

The carrier lifetimes obtained from Eq. (20) and Eq. (21) are plotted in Fig. 1 versus the neutron recoil energy for a 30 μm Zn granule. The relaxation processes are faster at high recoil energies due to the decrease of τ_e when the temperature T_∞ is increased.

The lifetime ratio derived in Eq. (20) differs from the expression used in previous works [10] where it was assumed that $\tau_p/\tau_e = C_p/C_{es}$ with the specific heats constant in temperature and evaluated at T_b. This approximation holds only at high bath temperatures where the relative temperature rise is small. At low temperatures where $C_{es} \ll C_p$, the values of τ_p evaluated from the ratio of the specific heats are many orders of magnitude bigger than τ_e.

4 Rise in temperature after a nuclear recoil

In order to study the rise in temperature on the granule surface after a nuclear recoil, we considered Sn and Zn granules with diameters 17 μm and 30 μm respectively. The granule dimensions were chosen according to the SSG detectors used in the irradiation experiments with a 70 MeV neutron beam [4].

The quasiparticle diffusivities in the superconducting state (D_e) were evaluated at the temperature T_∞ using the relation:

$$D_e = D_{en}\sqrt{\frac{2K_B T_\infty}{\pi \Delta_o}} \tag{22}$$

with the energy gap value Δ_o at $T = 0K$. The normal conducting diffusivities D_{en} were extrapolated from reference values [19] using the Wiedemann-Frantz law and the normal state electrical resistivity measured [20] on granules similar to the ones used in the neutron irradiation tests. Typical values at T=100 mK for D_e are $\sim 2 \cdot 10^{-4}$ m^2/s and $\sim 8 \cdot 10^{-4}$ m^2/s in Zn and Sn granules respectively.

The phonon thermal diffusivity is less than D_e and could not be extrapolated from measurements. We performed computations of the quasiparticle and phonon temperatures either neglecting D_p or with $D_p = D_e/100$ without obtaining substantial differences in the thermal diffusion process. The lifetimes τ_e and τ_p were evaluated at the temperature T_∞.

Nuclear recoils inside the granule, were simulated considering a three dimensional grid of equally spaced interaction points located in the half sphere with the coordinate ϕ in the interval $0 - \pi$. For each interaction point, the quasiparticle and phonon temperatures were calculated for a point on the granule surface located on the equator at $\phi = \pi/2$. The obtained temperature rises are plotted in Figs. 2 and 3 for a recoil energy of 10 keV deposited in Zn and Sn granules at the bath temperature of 50 mK.

In both Sn and Zn granules, the temperature rise on the granule surface depends on the location of the interaction point. After nuclear recoils located close to the middle of the granule, the deposited energy diffuses symmetrically as shown in Fig.

4(a). The granule surface is heated uniformly and the temperature rises smoothly from the bath to the equilibrium temperature T_∞ (lower curves in Figs. 2 and 3).

For interactions close to the surface the initial energy spreads in a small volume before reaching the surface as shown in Fig. 4(b). As a result, at the beginning of the diffusion process temperatures much higher than the final value T_∞ can be obtained in a small portion of the surface in both Sn and Zn granules (upper curves in Figs. 2 and 3). At the end of the diffusion, all the temperatures converge to the equilibrium value T_∞.

The time dependence of the quasiparticle and phonon temperatures is determined by the carriers lifetimes. The relaxation times in Sn for nuclear recoils of 10 keV, evaluated from Eq. (20) and Eq. (21), are $\tau_e \sim \tau_p$=1 ns. The energy exchange between the two systems occurs in a short time scale and the phonons and quasiparticle temperatures exhibit the same time dependence. In the case of Zn, the excited quasiparticles loose energy in a longer time scale than the phonons since τ_e=300 ns and τ_p=53 ns. At the beginning of the diffusion process a fraction of the initial energy is stored in the quasiparticle system and the quasiparticle temperature rise faster than the phonon temperature.

Due to the different values of the carrier lifetimes, the thermalization process is faster in Sn than in Zn. The temperature rise on the granule surface depends on the location of the interaction point and nuclear recoils close to the surface produce localized heating in Sn as well as in Zn granules. The quasiparticle relaxation times are responsible for the time scale of the diffusion process

5 Phase Transition

Irradiation experiments with SSG detectors are performed at a constant bath temperature biasing the detector with a magnetic field B_a less than the superheating field $B_{sh}(T_b)$. The quantity $h = 1 - B_a/B_{sh}(T_b)$ defines the magnetic threshold of the detector. Due to the Meissner effect, the strength of the applied magnetic field on the granule surface decreases with $\sin\theta$. At the equator the effective field has the maximum value $1.5B_a$ and it is zero at the poles.

After a particle interaction the deposited energy diffuses into the granule via phonons and quasiparticles. The phase transition is determined by the rise of the quasiparticle temperature on the granule surface which reduces the strength of the superheating field. The critical temperature $t_c^* = T_c^*/T_c$, needed to fulfill the condition on the granule surface $B_{sh}(t_c^*)=B_a \sin\theta$, is evaluated from the temperature dependence of the superheating field $B_{sh}(t)=B_{sh}(0)(1\text{-}t^2)$ and is:

$$t_c^* = \sqrt{1 - \sin\theta(1-h)(1-t_b^2)} \tag{23}$$

with t_b the reduced bath temperature. At low magnetic thresholds, the temperature T_c^* evaluated at angles $\theta \sim 70°$ is two times higher than the corresponding value on the equatorial plane.

In a global heating scenario, the phase transition is assumed to occur at the end of the thermalization process when the quasiparticle temperature reaches the equilibrium value T_e=T_p=T_∞. The most sensitive region of the granule is the equator where T_c^* has its minimum value. The maximum magnetic threshold h_m to produce a phase transition is then derived from the condition T_∞=$T_c^*(\theta$=$\pi/2)$ and it is:

$$h_m = \frac{T_\infty^2 - T_b^2}{T_c^2 - T_b^2} \tag{24}$$

where T_∞ is evaluated from Eq. (19) considering the specific heats of the phonon and superconducting electrons.

Although the phonon temperature is not directly responsible for the occurrence of the phase transition, the specific heat and the relaxation time of the phonon system play an important role in the energy diffusion inside the granule. Therefore the phonon contribution can not be neglected.

6 Sensitivity to nuclear recoils

For interactions localized in the middle of the granule, the heat diffuses symmetrically inside the granule as shown in Fig. 4(a). The quasiparticle temperature on the whole equator rises smoothly from the bath to the equilibrium temperature T_∞ and the phase transition occurs when $T_e \geq T_c^*(\theta$=$\pi/2)$. In this case, the maximum detector threshold is given by Eq. (24) as predicted by the global heating model.

Irradiation experiments with radioactive sources [6], minimum ionizing particles [5] and neutron beam [4] have shown that the sensitivity of Sn and In granules is higher than expected from the global heating model. These results suggest that the phase transition can occur also when a small portion of the granule surface, instead of the full equator, is heated above the threshold temperature. This local heating effect was found to be less evident in Zn and in Al granules.

Further measurements on single granules [6] without radioactive sources, have shown that the nucleation of the phase transition is sensitive to the orientation of the granule with respect to the magnetic field. The shape of the measured distributions of superheating fields were well reproduced considering three nucleation centers on the granule surface related not only to surface defects but also to the crystallographic orientation of the granule.

Since SSG detectors are made of a collection of granules ($\sim 10^6$) with a distribution of nucleation centers on the granule surface, it is quite difficult to define a criteria for the occurrence of the phase transition valid for all the granules inside the detector.

To evaluate the sensitivity of Sn and Zn granules to nuclear recoils, we considered a three dimensional grid of 122 equally spaced interaction points distributed in the whole granule volume. For each interaction point, the quasiparticle temperatures were monitored on three sets of points on the granule surface with time steps of 10

ns from 0 up to 400 ns in Sn and 1.5 μs in Zn. The phase transitions were produced requiring that the condition $T_e \geq T_c^*$ was simultaneously satisfied on the granule surface belonging to the same set.

The first set consisted of equally spaced points on the granule equator corresponding to the global heating scenario.

The second set was used to simulate the minimum surface area that has to be heated above the critical temperature T_c^* to nucleate the phase transition. The energy released in nuclear recoils close to the surface spreads asymmetrically and temperatures well above T_c^* can be reached in a small surface region near the interaction point. The critical size for this hot spot to produce a normal region and allow the field penetration (nucleation center) is related to the coherence length representing the characteristic length for the variation of the order parameter. Due to the $\sin\theta$ dependence of T_c^*, the location of the normal hot spot on the granule surface plays a role in the activation of the normal region as nucleation center for the phase transition.

The size of the second set of points on the granule surface was chosen to allow the penetration of the external field from the equator into the granule in the form of a tube of radius 0.2 μm and 1.2 μm in Sn and Zn respectively. The radius was chosen to be roughly equal to the coherence lengths in the two materials [21]. The third set was similar to the second but located on the opposite side of the granule.

The obtained sensitivities to 5 keV and 50 keV nuclear recoils of 17 μm Sn and 30 μm Zn granules are shown in Figs. 5 and 6. The histograms were generated recording, for each detector threshold and interaction point, only the transition occurring first in time in one of the three sets.

The calculated sensitivities of Sn and Zn granules have a sharp step at the magnetic threshold h_m evaluated from Eq. (24) corresponding to the global heating sensitivity. At thresholds below h_m, all the nuclear recoil interactions produce a phase transition and the detector sensitivity is not affected by the location of the interaction point.

At thresholds higher than h_m, the phase transitions are produced by interactions close to the surface. The size of the nucleation center is smaller in Sn than in Zn due to the different values of the coherence length. As a result, the reduced critical temperatures t_c^* needed to induce the phase transition is higher in Zn. A small fraction of nuclear recoils ($\sim$5%) produces phase transitions in Zn granules for $h \geq h_m$, where only interactions very close to the surface can be detected. The sensitivity of Sn granules is higher at thresholds above the global heating limit h_m because of the smaller thermal energy required to activate the nucleation center. For recoil energies of 50 keV an appreciable counting rate ($\sim$40%) can be obtained at thresholds two times higher than h_m.

The criteria used in the present work to define the occurrence of the phase transition does not take into account the dynamics of the field penetration. The minimum size of the nucleation center is deduced following geometrical considerations neglecting the variation of the Gibbs free energy due to the penetration of the applied field. Des-

pite these simplified assumptions, the calculations reproduce quite well the enhanced sensitivity measured in Sn SSG and the global heating sensitivity of Zn granules. The calculated histograms of Figs. 5 and 6 also reproduce the shape of the measured sensitivities of Sn and Zn granules to α particles (see Figs. 10 and 12 of Ref. [6]).

The agreement between calculations and measurements seems to suggest that the different sensitivity of Sn and Zn granules is mainly due to the thermal energy needed to start the nucleation of the phase transition and is not determined by the differences in the quasiparticle lifetimes. The quasiparticle relaxation times are responsible for the time scale of the diffusion process but have little effect on the dependence of the quasiparticle temperature on the location of the interaction point. Although there is almost a factor of hundred between the relaxation times in Sn and Zn, nuclear recoils close to the surface produce localized heating in Zn as well as in Sn granules (see Sec. 4).

The minimum surface area that has to be heated to produce a phase transition is smaller in Sn than in Zn due to the different values of the coherence lengths. As a result, Sn granules are more sensitive to interactions close to the surface depositing recoil energies below the global heating threshold.

In addition, the coherence lengths in Al and Zn are similar ($\sim$1 μm) and both materials show a global heating sensitivity while Sn and In granules have smaller coherence lengths ($\sim$0.2 μm) and in both materials the measured sensitivity to particle interactions is higher than predicted by the global heating model.

Sn and Zn detectors made of granules with diameters of $\sim$5 μm are planned for the proposed dark matter search with SSG [2]. These very small granules should exhibit only global heating, corresponding to well defined energy thresholds, since the granule dimensions become comparable with the minimum size of the nucleation center.

7 Delay in time between neutron recoils and phase transitions

To evaluate the time elapsing from the nuclear recoil to the nucleation of the phase transition, we monitored the quasiparticle temperatures in 30 μm Zn and 17 μm Sn granules. To compare with the neutron irradiation measurements [8], the temperatures were evaluated at three recoil energies in the ranges 5-15 keV and 40-60 keV in Zn and 40-60 keV in Sn.

The nuclear recoils were simulated considering a grid of 122 equally spaced points distributed inside the granules and the phase transition was determined using the criteria discussed in the previous section. For each interaction point, only the transition occurring first in time was considered. The calculated delay time distributions were weighted with the corresponding neutron elastic scattering cross sections and with the detection efficiency of the neutron counter used in the experiments. The distributions

belonging to the same range of recoil energies were added together. The probability distribution of the critical temperature T_c^*, due to the measured superheating field spread, was evaluated using a gaussian parameterization of the superheating field distribution.

In Figs. 7 and 8, the calculated distributions of the time delay between nuclear recoils and phase transitions are compared with the measurements taken from Ref. [8]. Despite the simplified assumptions, the calculations reproduce well the general features of the experimental results. It is important to note that the measured distributions have a constant time offset due to electronic delays, as discussed in Ref. [8], and only the relative time delay should be considered.

In the case of Zn granules, there is a difference in the shape of the calculated distributions for recoil energies in the ranges 5-15 keV and 40-60 keV. Since the quasiparticle thermal energies are higher at recoil energies of 40-60 keV, the Zn granules are more sensitive to interactions close to the surface and the theoretical distribution is shifted toward shorter times in agreement with the measurements as shown in Fig. 7. In Sn, the quasiparticle relaxation times are shorter and both the calculated and measured time delay distributions are within 150 ns.

8 Conclusions

We derived an analytical expression for the quasiparticle and phonon temperatures describing the heat propagation inside superconducting granules after particle interactions.

The calculations differ from previous works not only because the initial excitation is distributed in both quasiparticle and phonon systems, but also in the definition of the effective carrier lifetimes and initial temperatures. The derived expressions for the quasiparticle and phonon temperatures are valid for a point source located anywhere inside the superconducting granule.

The global or local heating sensitivity of SSG detectors to nuclear recoils was discussed considering the details of the energy propagation inside 17 μm Sn and 30 μm Zn granules. The occurrence of the phase transition was deduced using a simplified criteria to evaluate the minimum surface area that has to be heated above the critical temperature to nucleate the phase transition. The calculations reproduce well the enhanced sensitivity measured with Sn granules and the global heating sensitivity of Zn SSG.

The agreement between calculations and measurements seems to suggest that the observed difference in the sensitivity of Sn and Zn granules to nuclear recoils is mainly due to the thermal energy needed to start the nucleation of the phase transition and is not determined by the differences in the relaxation times of the two materials. Although there is almost a factor of hundred between the relaxation times in Sn and Zn, nuclear recoils close to the surface produce localized heating in Zn as well as in Sn granules. The temperature rise on the granule surface depends on the location of

the interaction point. The quasiparticle relaxation times are responsible for the time scale of the diffusion process.

The elapsed time from the nuclear recoil interaction to the nucleation of the phase transition was calculated for Sn an Zn granules. The calculations reproduce well the general features of the distributions measured in irradiation tests of SSG with a 70 MeV neutron beam.

The derived expressions for the quasiparticle and phonon temperatures are useful to predict the sensitivity of SSG detectors to nuclear recoils produced in dark matter particles or neutrinos interactions. The obtained expressions can also be used to study the energy diffusion after ionizing interactions where an important fraction of the initial energy is deposited close to the interaction point (i.e. soft x-rays absorption or neutrino nuclear interactions).

Acknowledgments

I would like to thank K. Pretzl and K. Schmiemann from the University of Bern for helpful discussions. This work was supported by the Schweizerischer Nationalfonds zur Foerderung der wissenschaftlichen Forschung.

References

[1] K. Pretzl, Particle World **1/6** 153 (1990); K. Pretzl, J. Low. Temp. Phys. **93/3** 439 (1993).

[2] M. Abplanalp et *al.*, J. Low. Temp. Phys. **93/3** 809 (1993).

[3] A. Gabutti and K. Schmiemann, Phys. Lett. B **308** 411 (1193).

[4] C. Berger et *al.*, Nucl. Instrum. and Methods A **330** 285 (1993); M. Abplanalp et *al.*, J. Low. Temp. Phys. **93/3** 491 (1993); M. Abplanalp et *al.*, Preprint Bern BUHE-94-5, submitted to Phys. Rev. D (July, 1994).

[5] G. Czapek et *al.*, Nucl. Instrum and Methods A **306** 572 (1991).

[6] M. Frank et *al.*, Nucl. Instrum and Methods A **287** 583 (1990).

[7] M. Frank et *al.*, Phys. Rev. B **43/7** 5321 (1991).

[8] M. Abplanalp et *al.*, Preprint Bern BUHE-94-1, to be published in *Superconductivity and Particle Detection*, proceedings of the International Workshop, April 20-24, 1994, Toledo, Spain, edited by G. Waysand (World Scientific Pub.).

[9] K. Gray in *Superconductive particle detectors*, proceedings of the Workshop, Turin, Italy, edited by A. Barone (World Scientific, Singapore, 1987) p.1.

[10] N. Perrin, J. Physique **47** 1939 (1986).

[11] V. Narayanamurti et *al.*, Phys. Rev. B **18/11** 6041 (1978).

[12] E.T. Swartz and R.O. Pohl, Rev. Mod. Phys. **61/3** 605 (1989).

[13] P.M. Morse and H. Feshbach, *Methods of theoretical physics*, (McGraw-Hill Book Company, New York, 1953) p. 1468.

[14] J. Lindhard et *al.*, Mat. Fys. Medd. Dan. Vid. Selsk. **33/10** 1 (1963).

[15] G. Gerbier et *al.*, Phys. Rev. D **42/9** 3211 (1990) ; T. Shutt et *al.*, Phys. Rev. Lett. **69/24** 3425 (1992).

[16] R.S. Raghavan, Phys. Rev. Lett. **37** 259 (1976).

[17] S.B. Kaplan et *al.*, Phys. Rev. B **14/11** 4854 (1976).

[18] M. Tinkham, *Introduction to Superconductivity* (Robert E. Krieger Publ. Company, Malabar, 1975)

[19] *Thermal conductivity*, edited by Y.S. Touloukian, R.W. Powell, C.Y. Ho and P.G. Klemens, (IF/Plenum, New York, 1970).

[20] M. Furlan et *al.*, Nucl. Instrum and Methods A **338** 544 (1994).

[21] J. Feder and D.S. McLachlan, Phys. Rev. **177/2** 763 (1969); K.S. Wood and D. Van Vechten, Nucl. Instrum and Methods A **314** 86 (1992).

Figure Captions

Fig. 1: Carrier lifetimes τ_e and τ_p versus recoil energy calculated from Eq. (19) and Eq. (20) for a 30 μm Zn granule at the bath temperature of 50 mK. The ionization ratio f is evaluated from Eq. (17).

Fig. 2: Calculated quasiparticle (a) and phonon (b) temperatures versus time for 10 keV nuclear recoils in a 30 μm Zn granule. The interactions were distributed in a three dimensional grid of equally spaced points located inside the half sphere ϕ=0-π. The temperatures were monitored on the granule equator at the point $\phi=\pi/2$.

Fig. 3: As in Fig. 2. Calculated quasiparticle (a) and phonon (b) temperatures for 10 keV nuclear recoils in a 17 μm Sn granule.

Fig. 4: 30 μm Zn granule at the bath temperature of 50 mK. Isothermal quasiparticle temperature profiles in the equatorial plane 120 ns after a 10 keV nuclear recoil close to the middle of the granule (a) and 1 μm from the surface (b). Full line T_e=650 mK, dashed line T_e=450 mK and dotted line T_e=250 mK. The outermost circle is the granule equator. In Sn granules, there is the same dependence of T_e on the location of the interaction point.

Fig. 5: Calculated number of phase transitions versus the magnetic threshold h for a 30 μm Zn granule at T_b=50 mK after 5 keV (a) and 50 keV (b) nuclear recoils. The interactions were distributed in a three dimensional grid of 122 equally spaced points located inside the granules. The distributions have a sharp step corresponding to the global heating threshold defined in Eq. (23).

Fig. 6: As in Fig. 5 for a 17 μm Sn granule after 5 keV (a) and 50 keV (b) nuclear recoils.

Fig. 7: Calculated (a,b) and measured (c,d) [8] distributions of the elapsed time from nuclear recoils to phase transitions in the case of a Zn SSG detector at the magnetic threshold h=0.02. The measured distributions have a constant offset due to electronic delays and only the relative time delay should be considered. The ranges of nuclear recoils are 5-15 keV (a,c) and 40-60 keV (b,d).

Fig. 8: As in Fig. 7. Calculated (a) and measured (b) [8] distributions for a Sn SSG detector exposed to nuclear recoils in the range 40-60 keV at the magnetic threshold h=0.01.

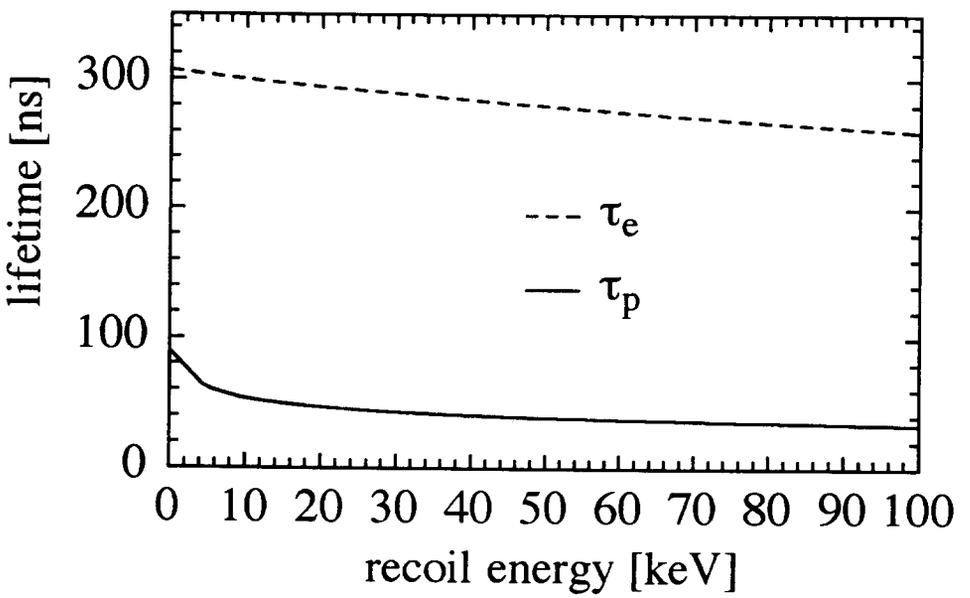
lifetime [ns]
300
200
100
0
--- τ_e
— τ_p
0 10 20 30 40 50 60 70 80 90 100
recoil energy [keV]

Fig.1 Fig.1

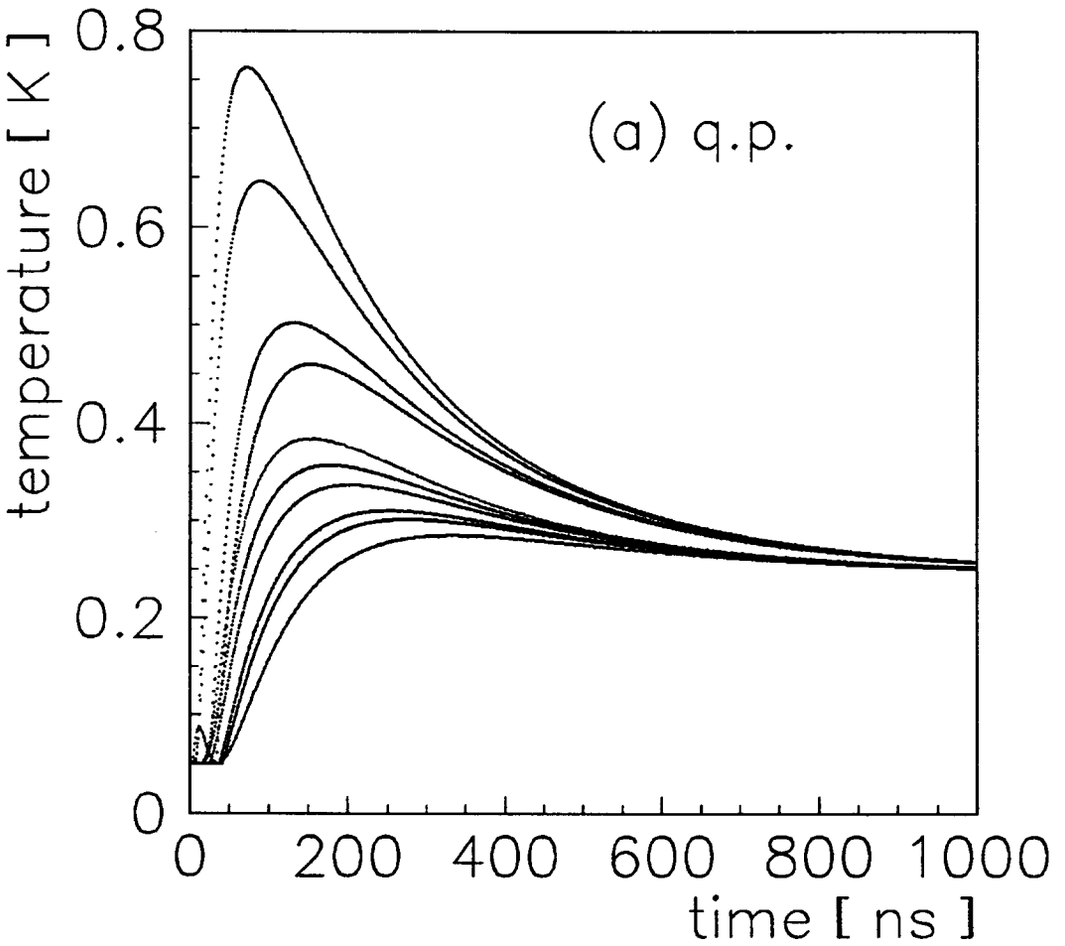

Fig.2a

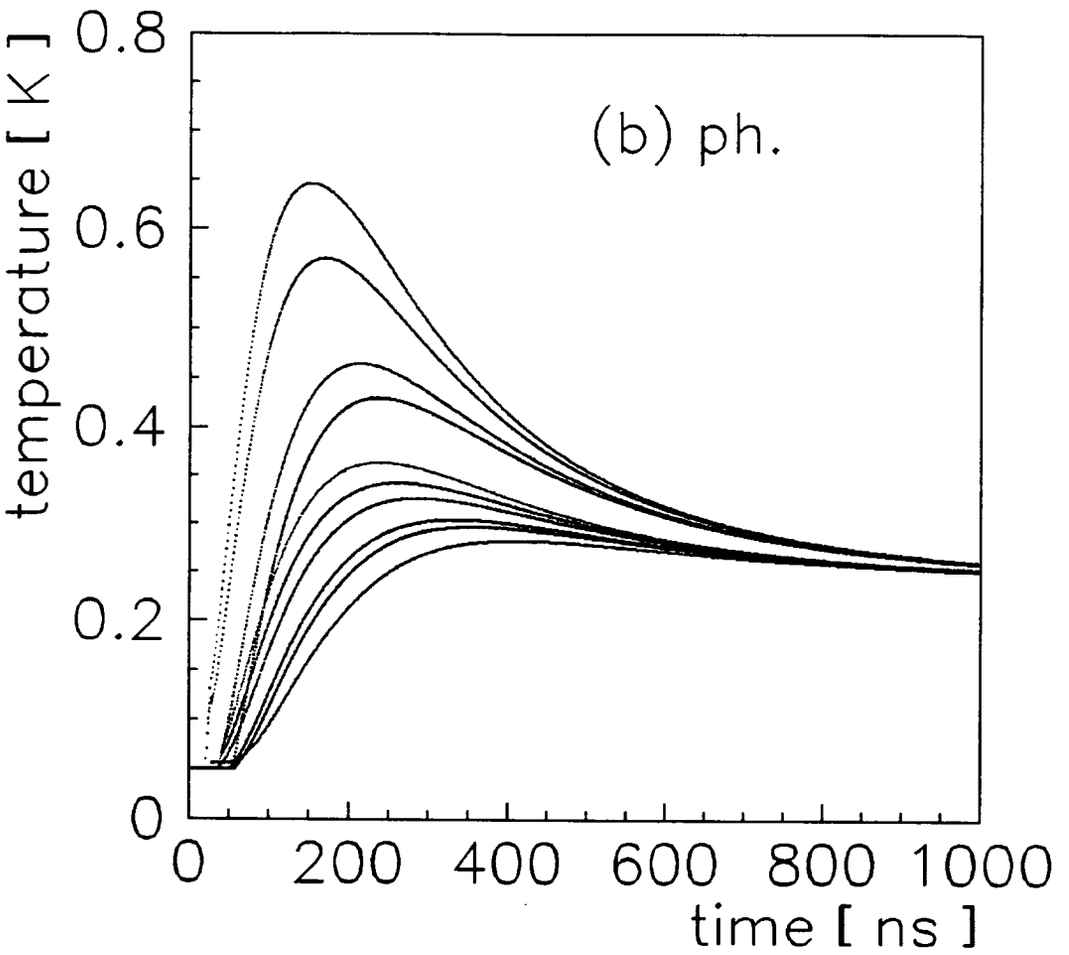

Fig.2b

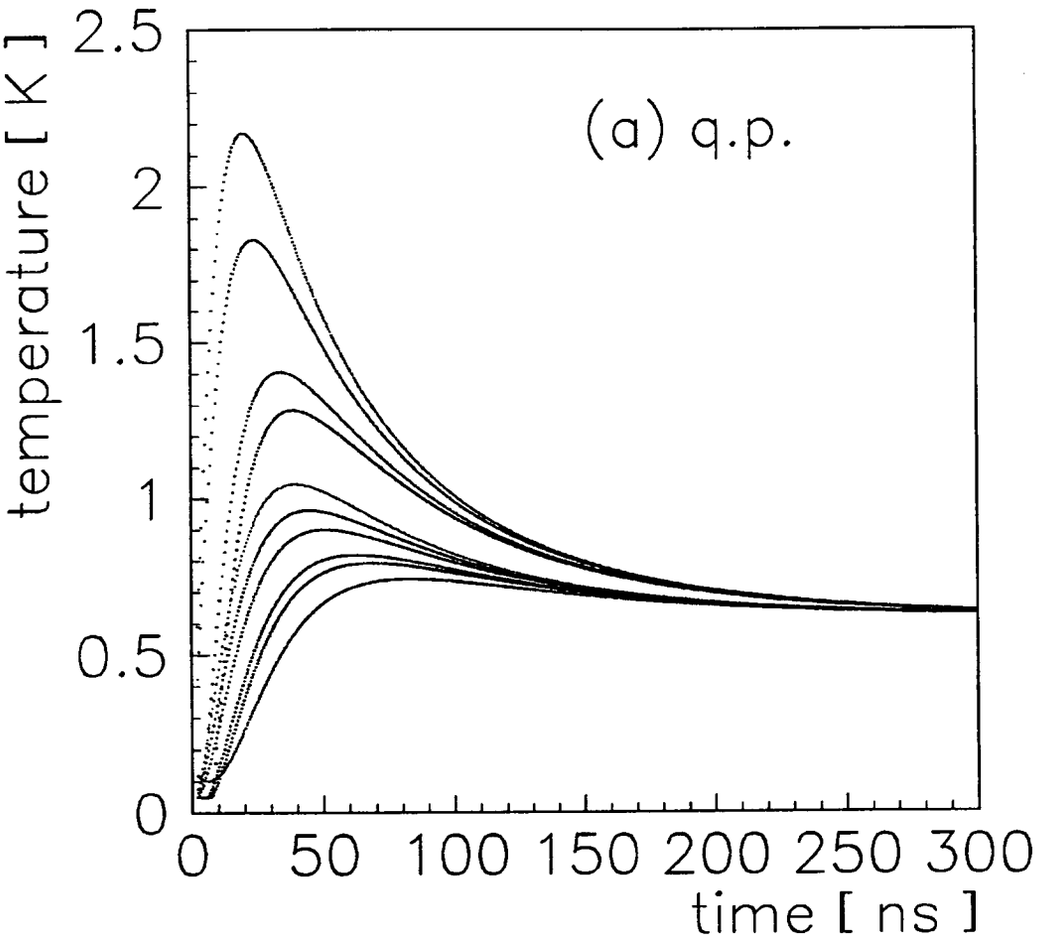

Fig.3a

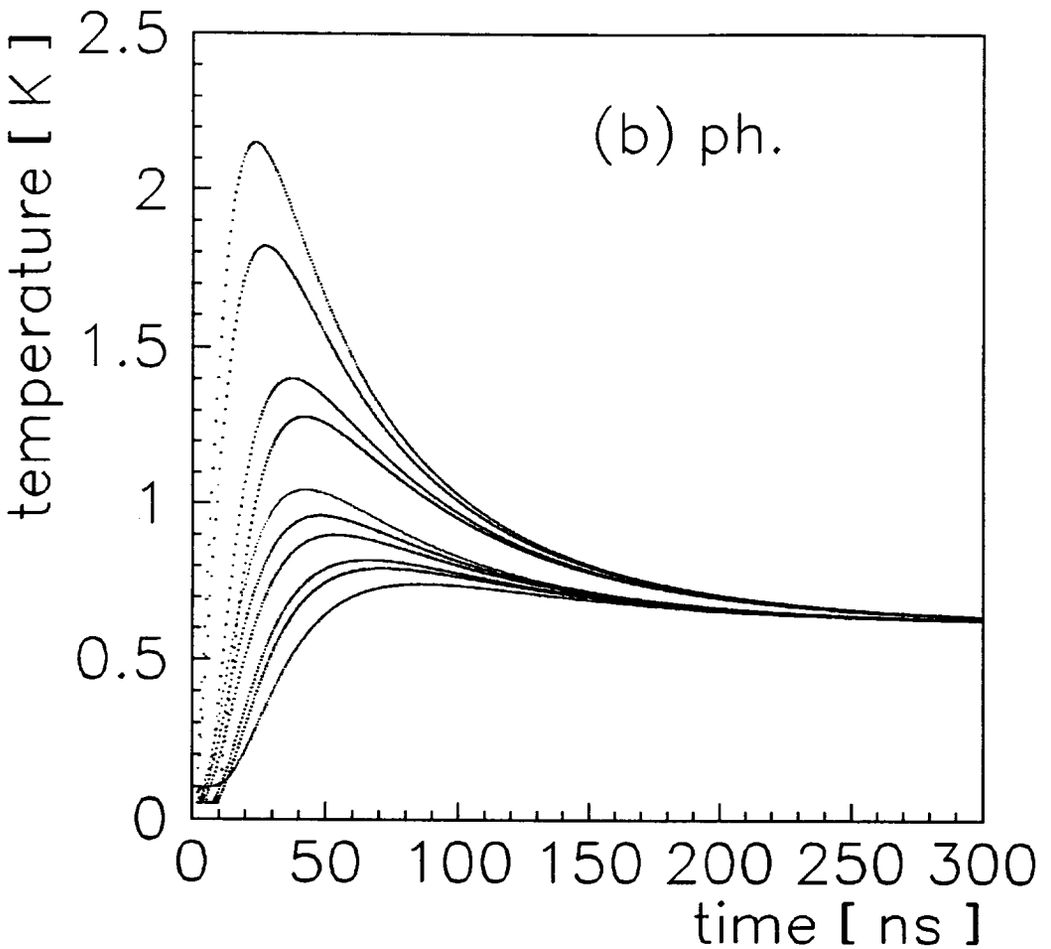

Fig.3b

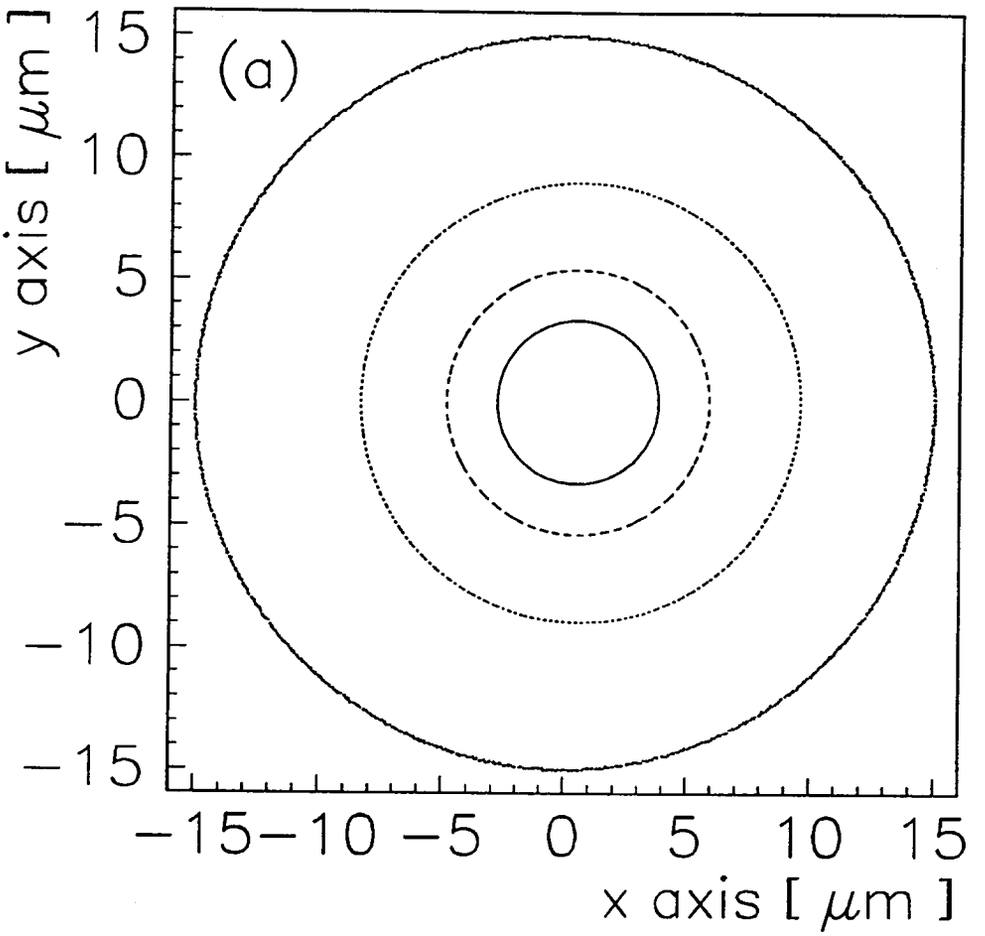

Fig.4a

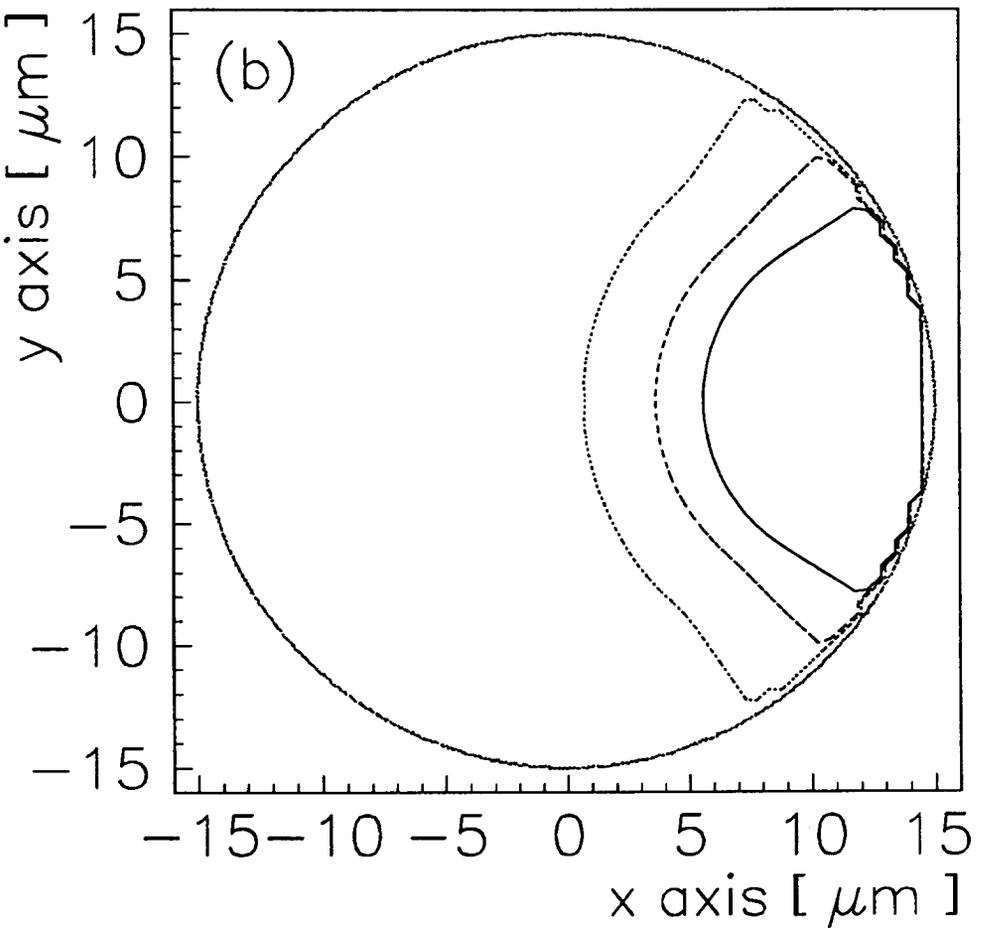

Fig.4b

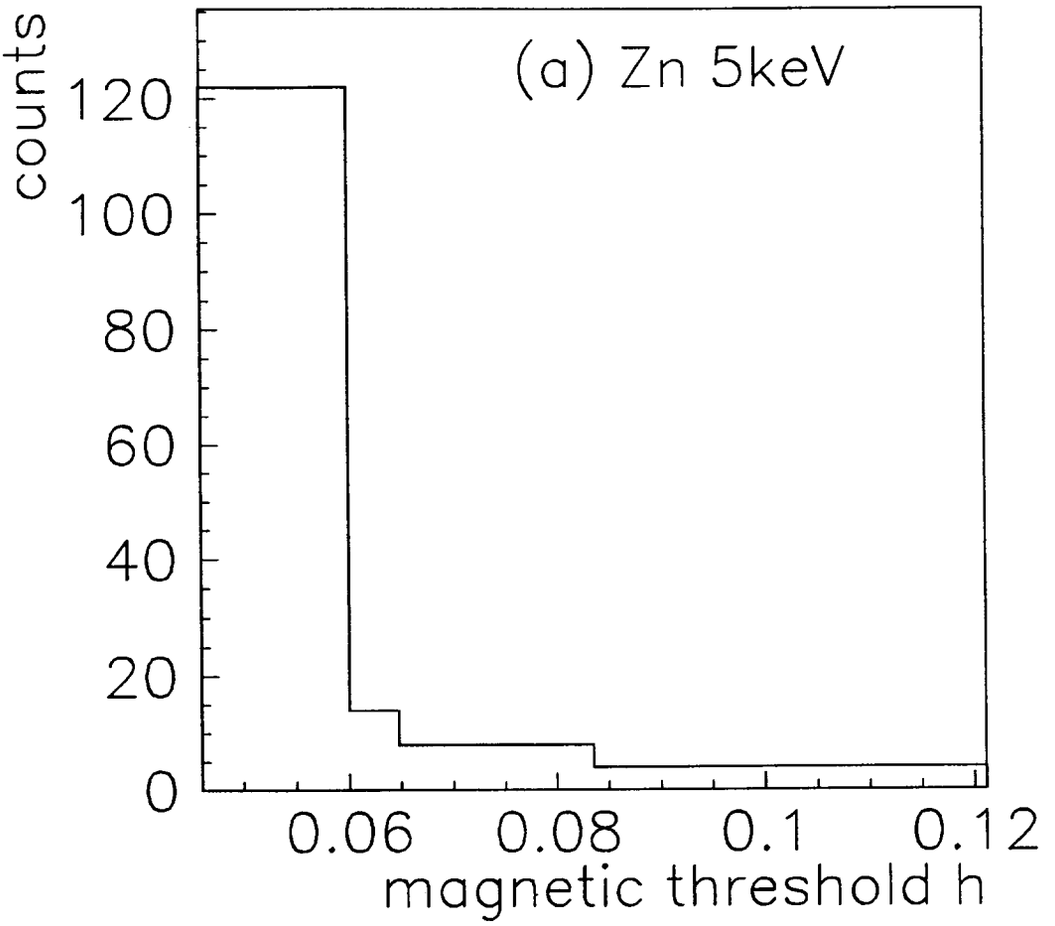
(a) Zn 5keV
counts
120
100
80
60
40
20
0
0.06
0.08
0.1
0.12
magnetic threshold h

Fig.5a

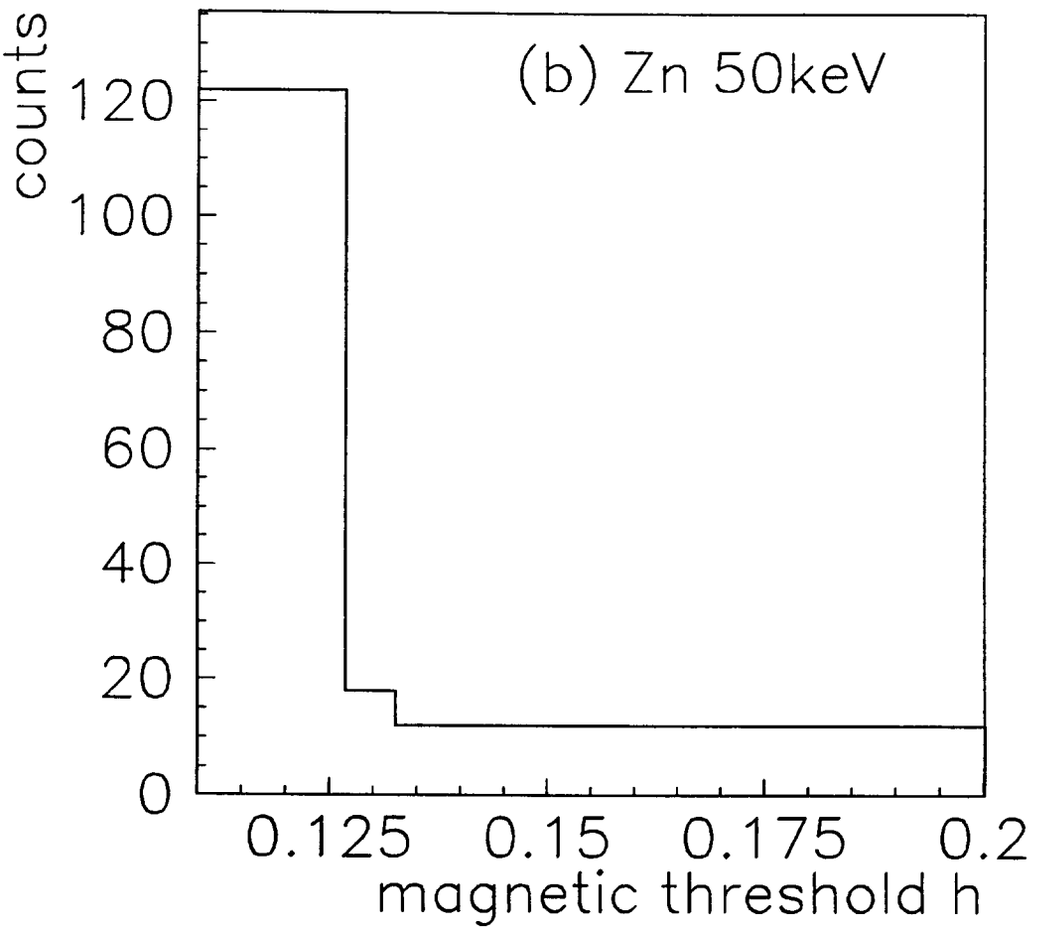
(b) Zn 50keV
counts
120
100
80
60
40
20
0
0.125
0.15
0.175
0.2
magnetic threshold h

Fig.5b

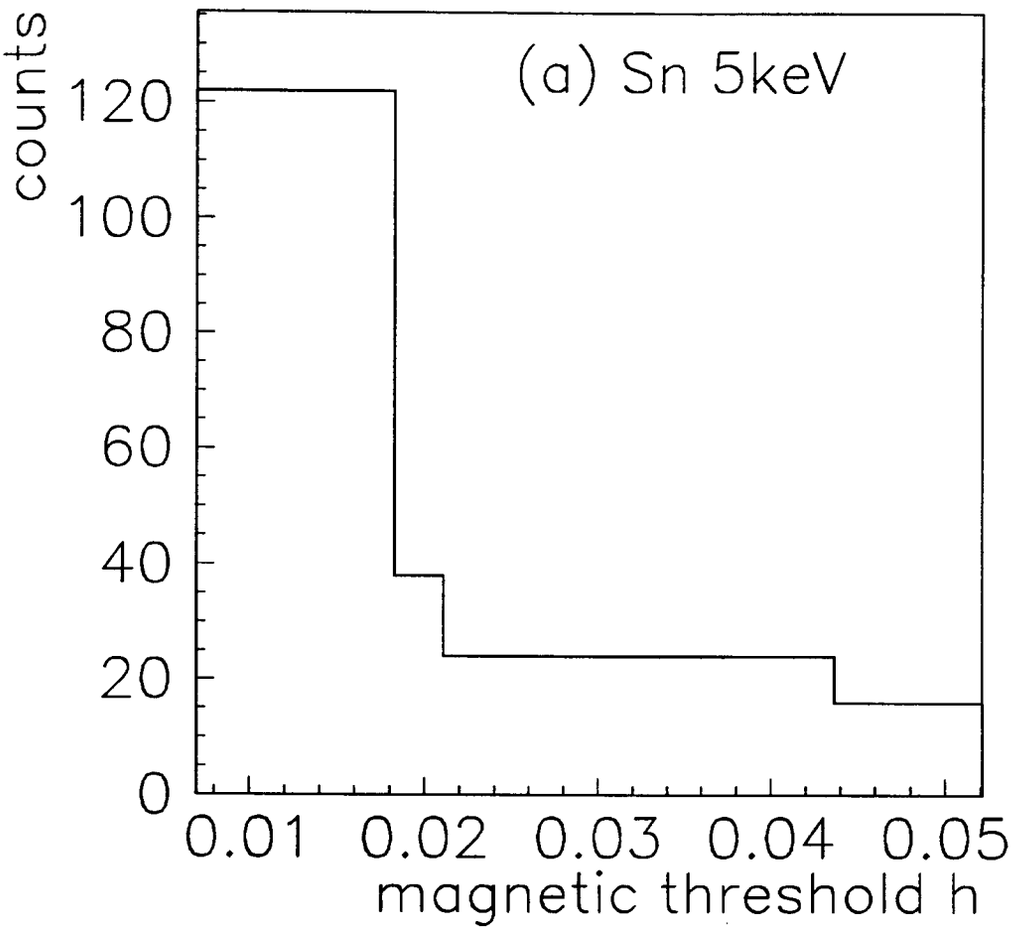
(a) Sn 5keV
counts
120
100
80
60
40
20
0
0.01
0.02
0.03
0.04
0.05
magnetic threshold h

Fig.6a

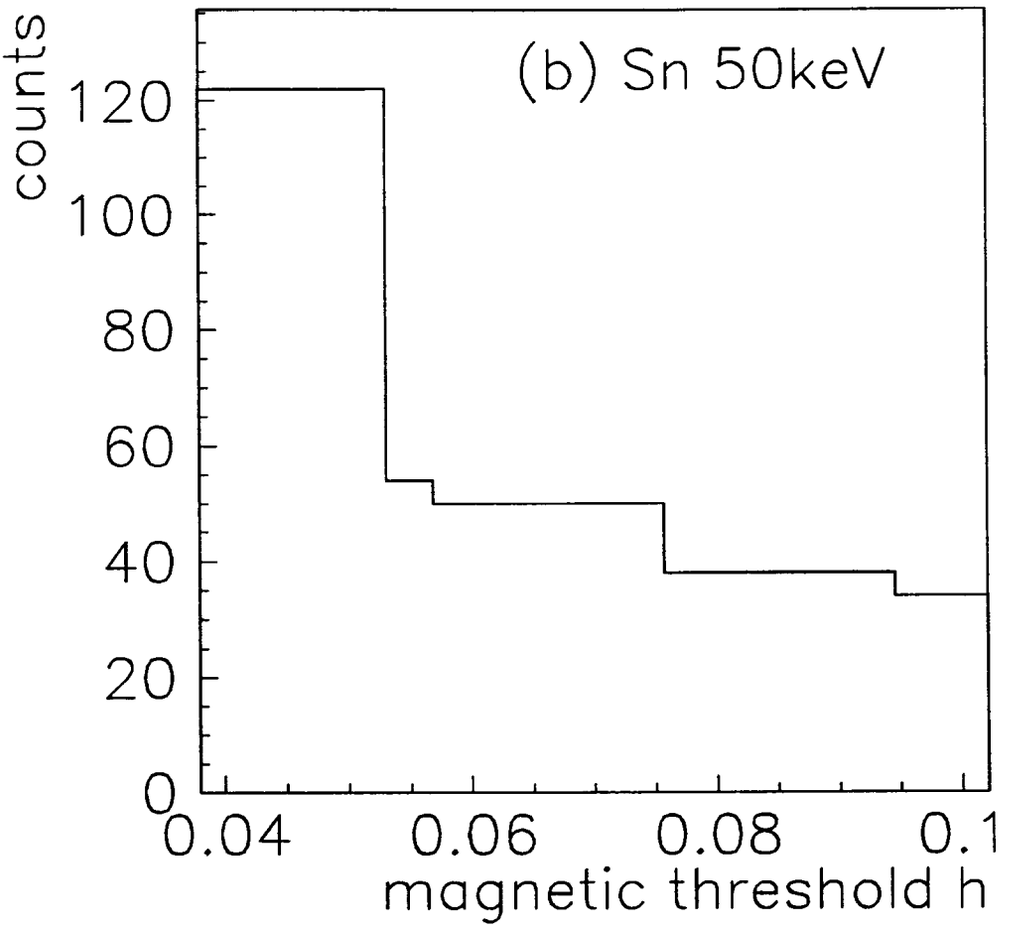
(b) Sn 50keV
counts
120
100
80
60
40
20
0
0.04
0.06
0.08
0.1
magnetic threshold h

Fig.6b

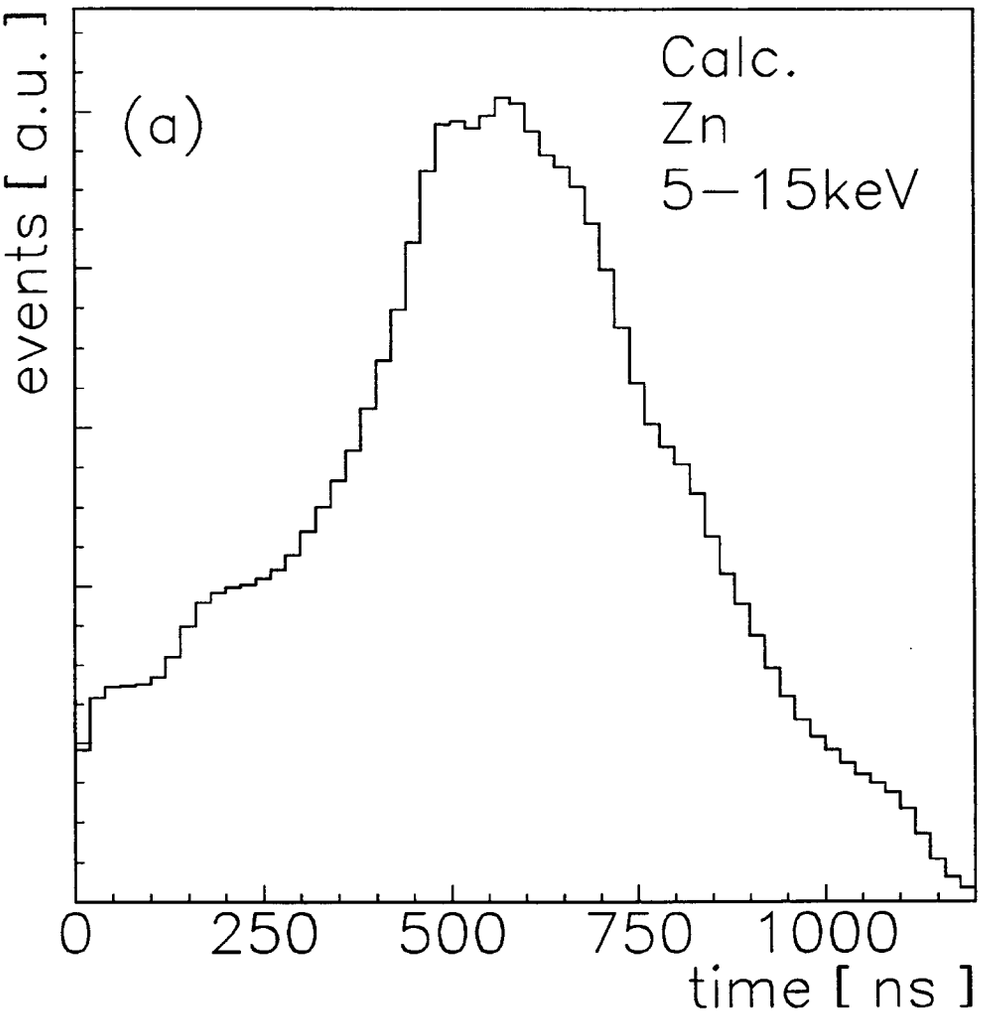

Fig.7a

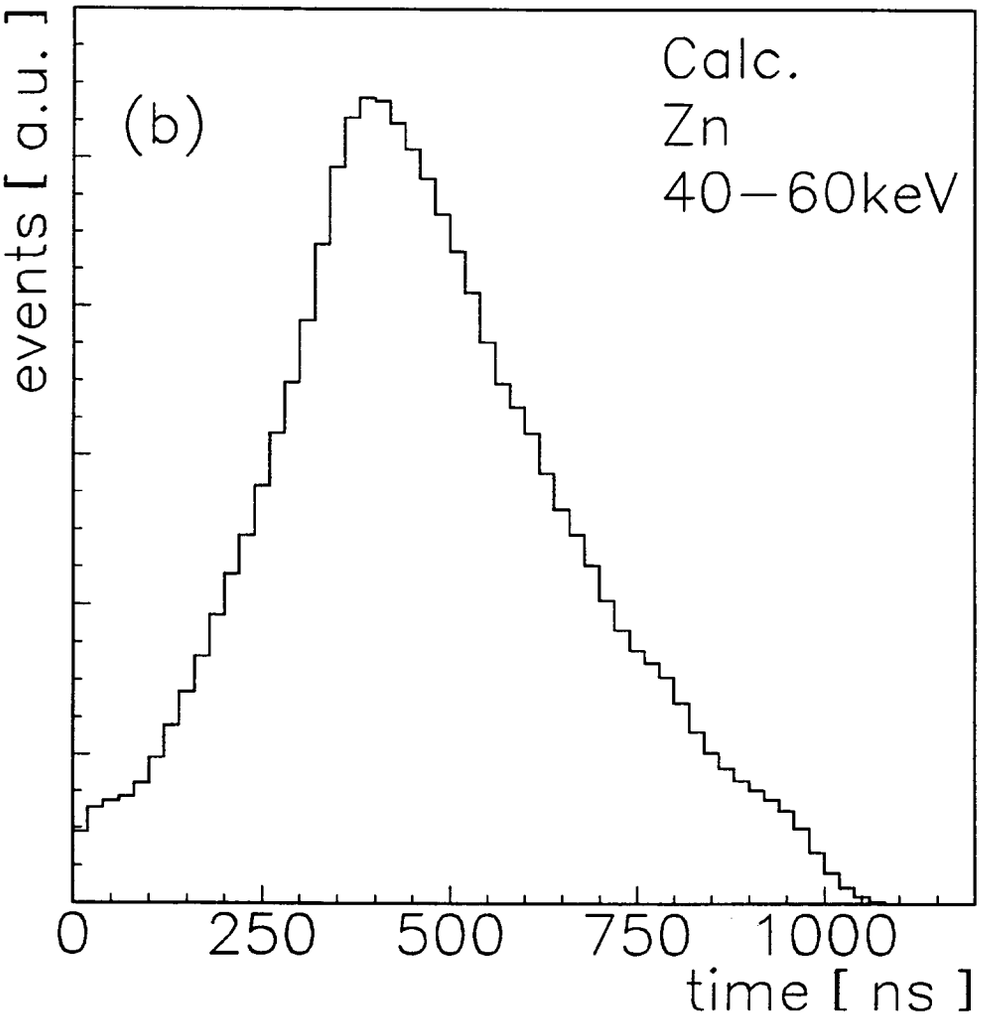

Fig.7b

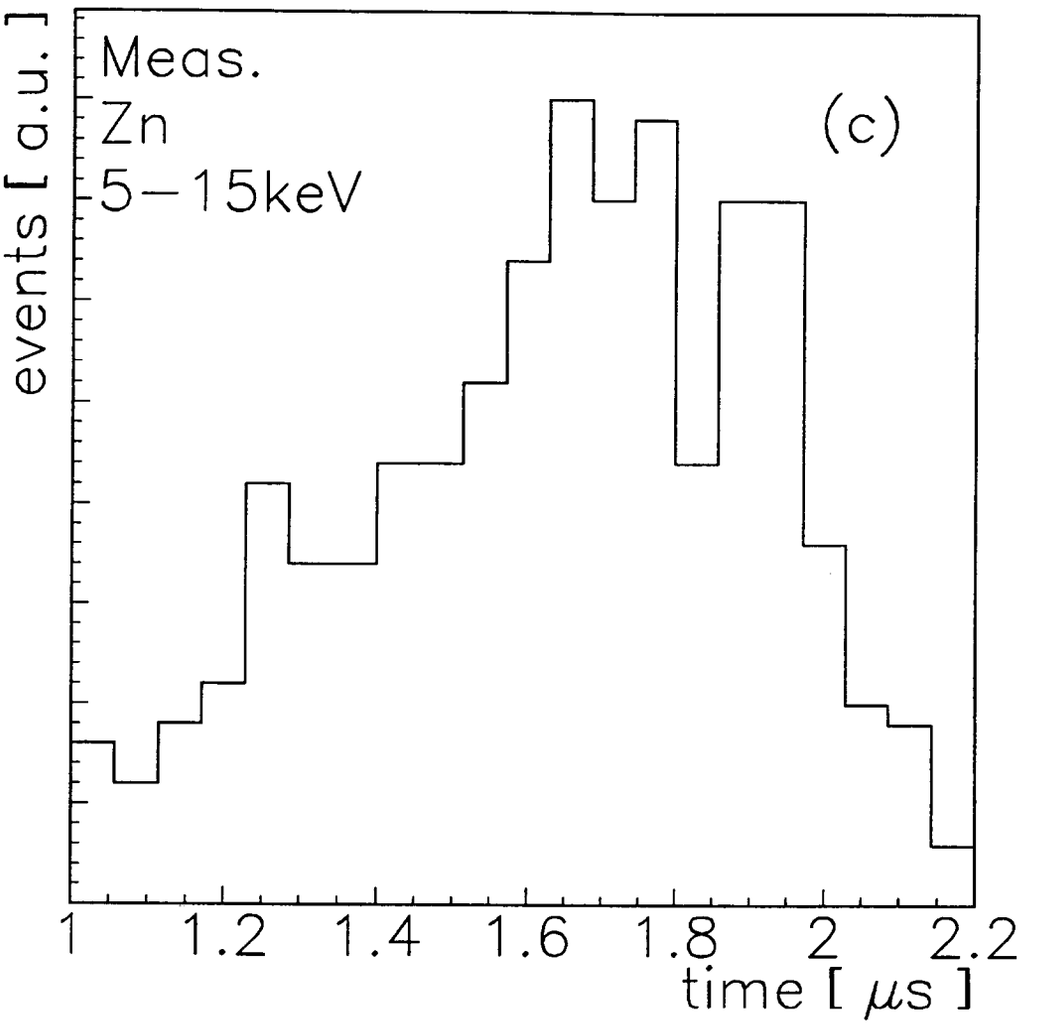

Fig.7c

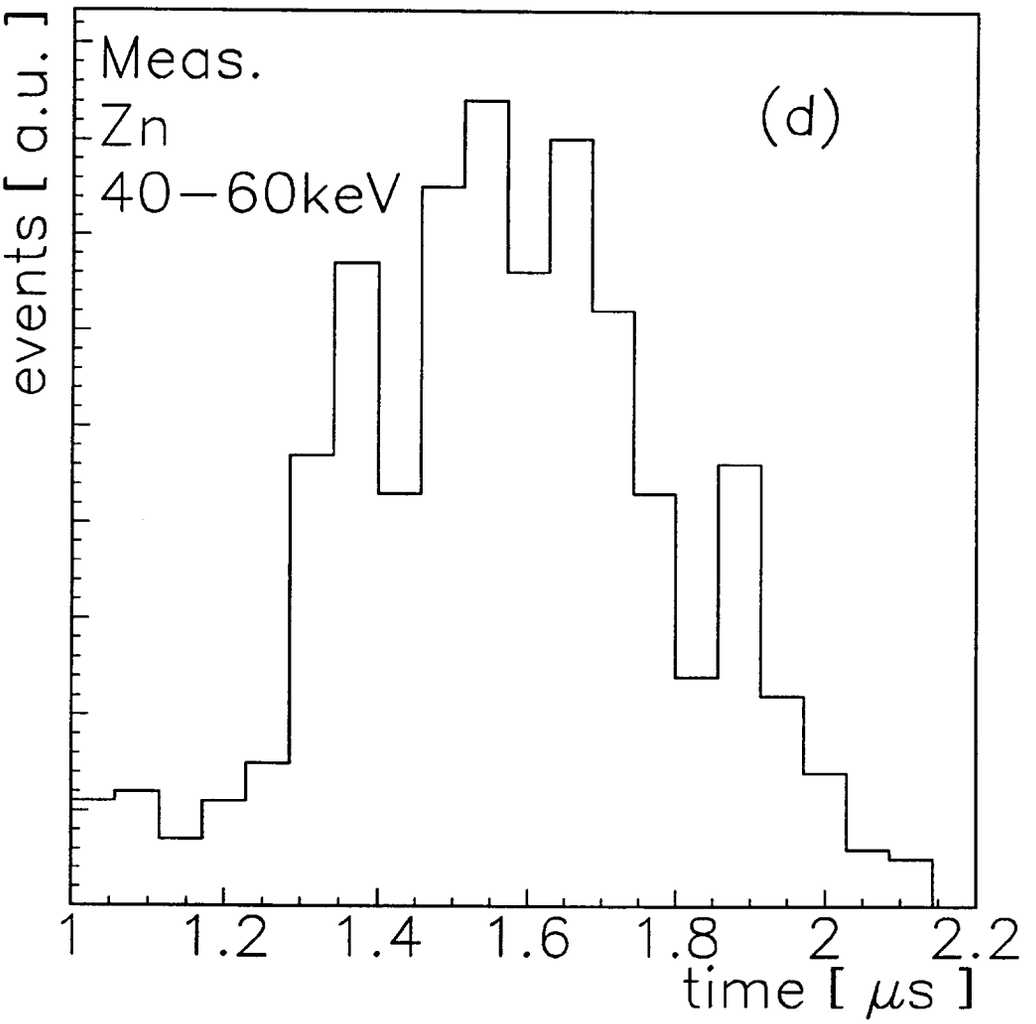

Fig.7d

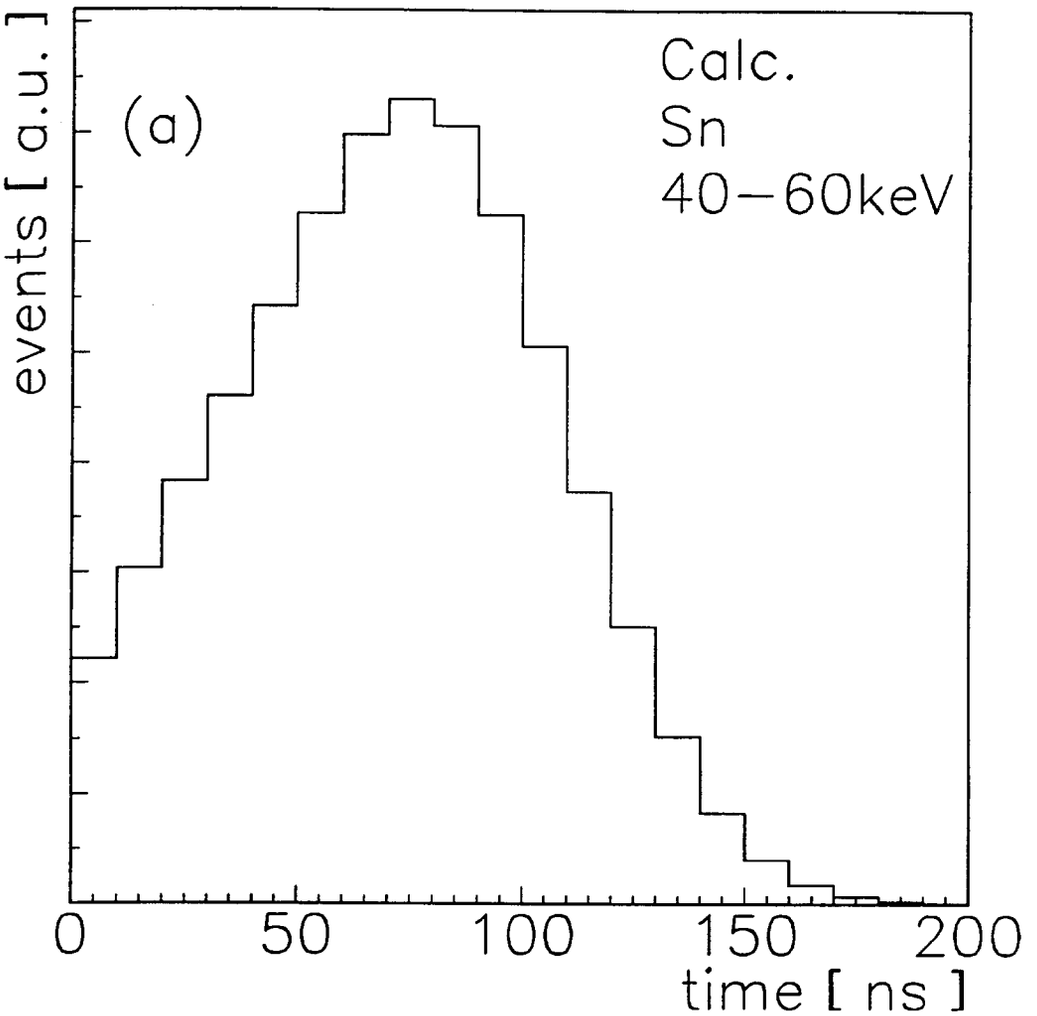

Fig.8a

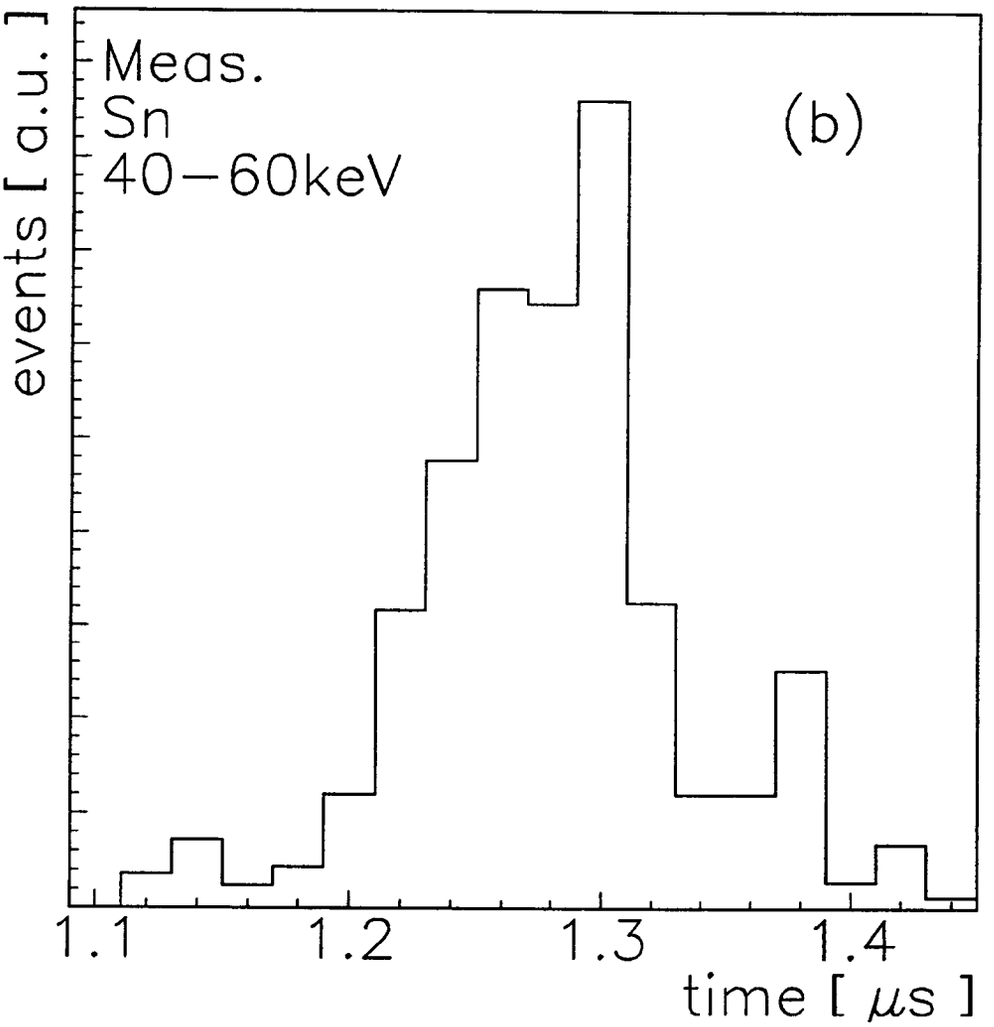

Fig.8b